Supplemental data

Supplemental figure S1

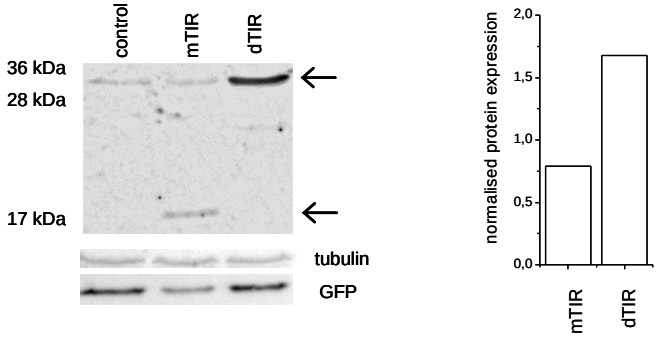

Figure S1: mTIR and dTIR exhibit comparable protein expression levels. HEK293T cells were transfected with control, mTIR or dTIR (3,5 μg) together with GFP (20 ng) plasmid. Proteins from cell lysates were separated on SDS-PAGE and immunoblotted using antibodies against MyD88 (for constructs), GFP and tubulin. The expected sizes for dTIR (35 kDa) and mTIR (17 kDa) are shown by arrows. dTIR band has about twice the intensity of the mTIR due to the duplication of the binding epitopes for antibodies against MyD88 used (left). Western blot bands of mTIR and dTIR were quantified and normalized against the levels of GFP (right).

Supplemental figure S2

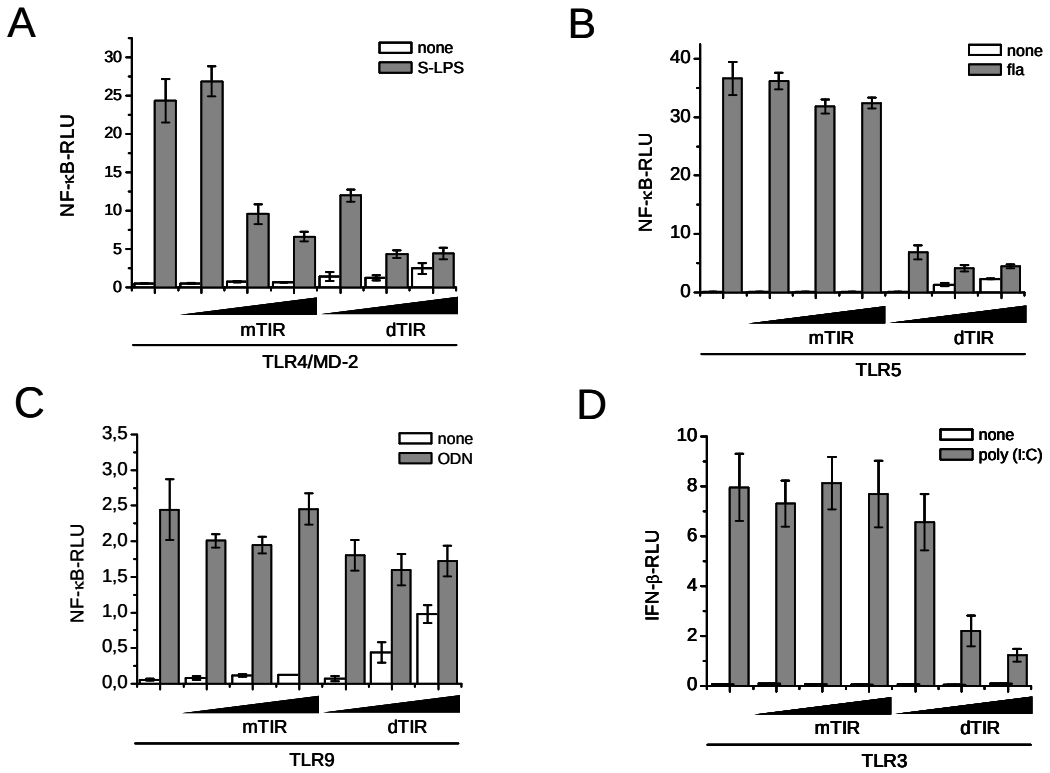

Figure S2: TLR activation in the absence of stimulation for the inhibition experiments with dTIR. Data represented on A-D represent the RLUs of unstimulated and stimulated cells and correspond to the experiments shown on Fig. 1, B-E.

Supplemental figure S3

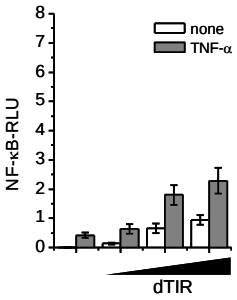

Figure S3: dTIR does not inhibit activation by TNF-α. HEK293 cells were transfected with dTIR plasmid (1 ng, 5 ng, 20 ng) and stimulated with TNF-α (250 ng/mL). Activation of TLR signaling pathway was determined by the dual luciferase assay. Data represent the RLUs of unstimulated and stimulated cells. Representative graph from three separate experiments is shown. Data on graphs are represented as mean +/- s.d..

Supplemental figure S4

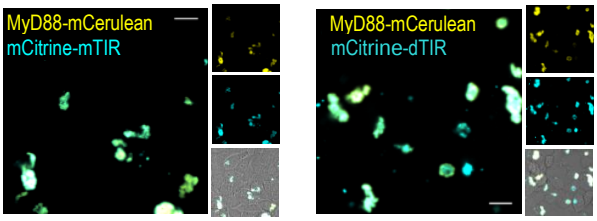

Figure S4: YFP-mTIR and YFP-dTIR co-localize with MyD88. HEK293T cells were transfected with MyD88-CFP (10 ng) and YFP-mTIR or YFP-dTIR (5 ng each). YFP-tagged constructs (cyan); MyD88-CFP (yellow). Representative micrographs are shown from three separate experiments. Scale bars on micrographs represent 10 μm.

Supplemental figure S5

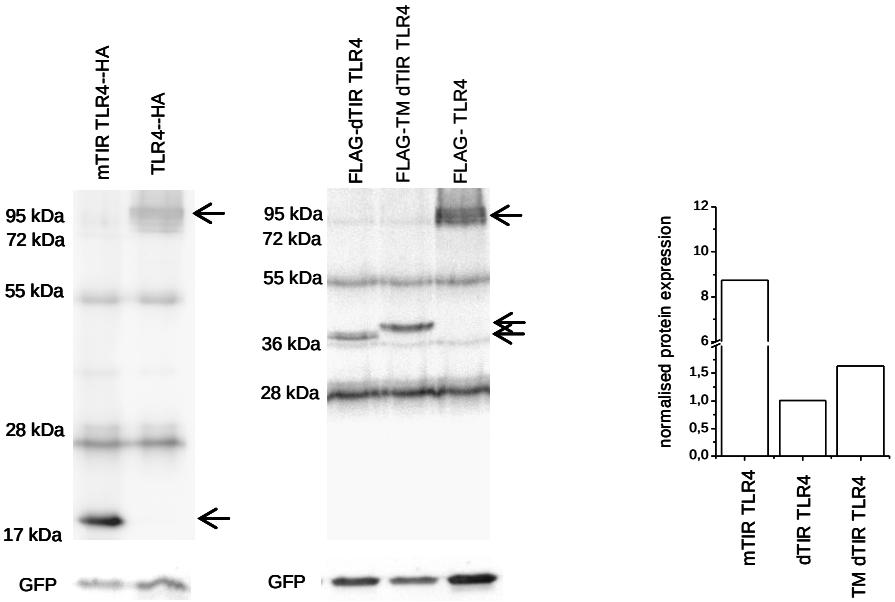

Figure S5: Protein expression of constructs containing TIR domain of TLR4. HEK293T cells were transfected with mTIR TLR4, dTIR TLR4, TM dTIR TLR4, HA-TLR4 or FLAG-TLR4 (3,5 µg) together with GFP (20 ng) plasmid as a transfection control. Proteins were immunoprecipitated from an equal amount of total proteins in cell lysate, separated on SDS-PAGE and immunoblotted using antibodies against HA tag, FLAG tag and AU-1 tag. The arrows indicate the positions of TLR4-HA (97 kDa), and mTIR TLR4 on the left panel and FLAG-TLR4 (97 kDa), TM dTIR TLR4 (40 kDa) and dTIR TLR4 (38 kDa) on the middle panel, from top to bottom, respectively. Western blot bands were quantified and normalised against the levels of GFP and represented relative to the expressed TLR4 (right panel).

Supplemental figure S6

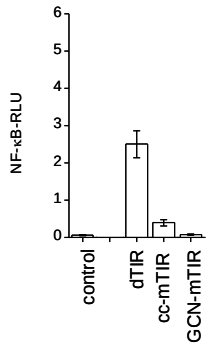

Figure S6: Coiled-coil segment prevents constitutive activation of TIR dimers. HEK293 cells were transfected with control, dTIR, cc-mTIR or GCN-mTIR (20 ng). Activation of TLR signaling pathway was determined by the dual luciferase assay. Representative graph is shown from three separate experiments. Data on graphs are represented as mean +/- s.d..

Supplemental figure S7

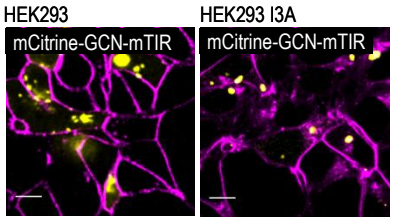

Figure S7: GCN-mTIR localizes similar to but independently of MyD88. HEK293T or HEKI3A cells were transfected with YFP-GCN-mTIR (10 ng). GCN-mTIR (yellow); SynaptoRed (magenta). Representative micrographs are shown from three separate experiments. Scale bars on micrographs represent 10 μm.

Supplemental figure S8

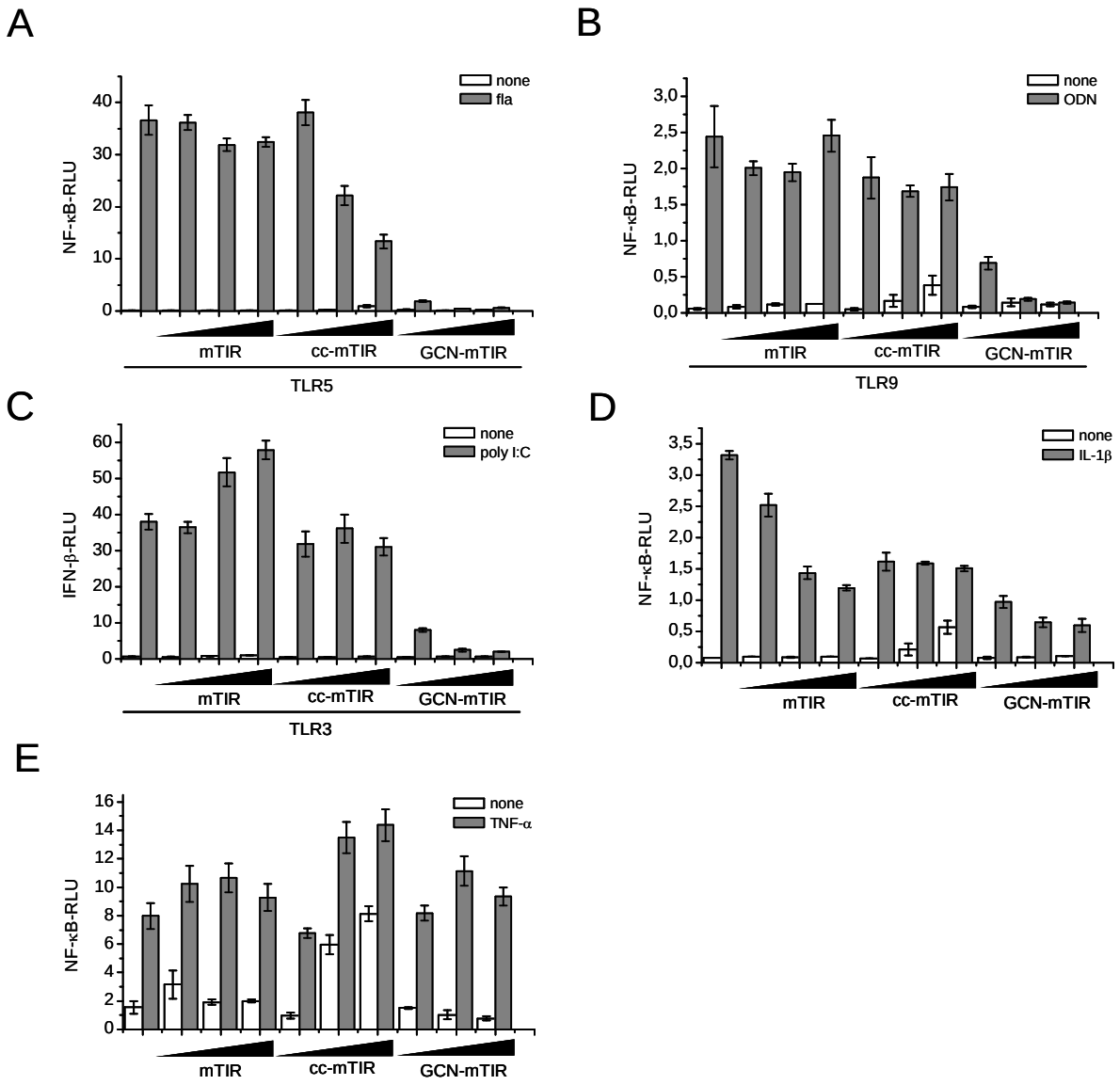

Figure S8: The amount of activation in the absence of stimulation for the experiments of improved TLR inhibition with cc-mTIR and GCN-mTIR. Data represented on A-E represent the RLUs of unstimulated and stimulated cells and correspond to the experiments shown on Fig. 5 A-C, E, F.

Supplemental figure S9

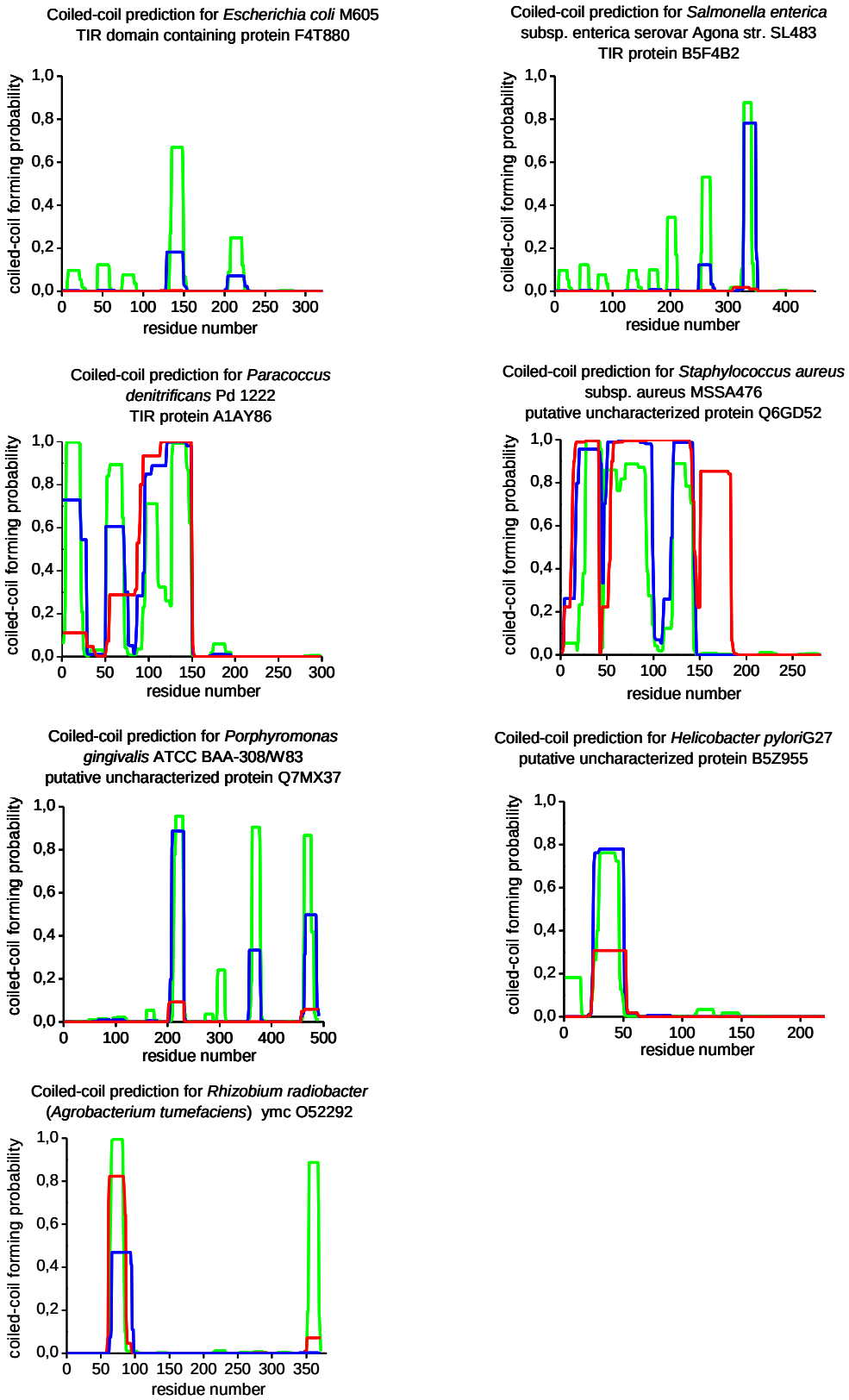

Figure S9: Predictions of a coiled-coil formation within different bacterial TCPs.

The coiled-coil-forming propensity is presented for frames of 14 (green), 21 (blue) and 28 (red) residues.

Supplemental figure S10

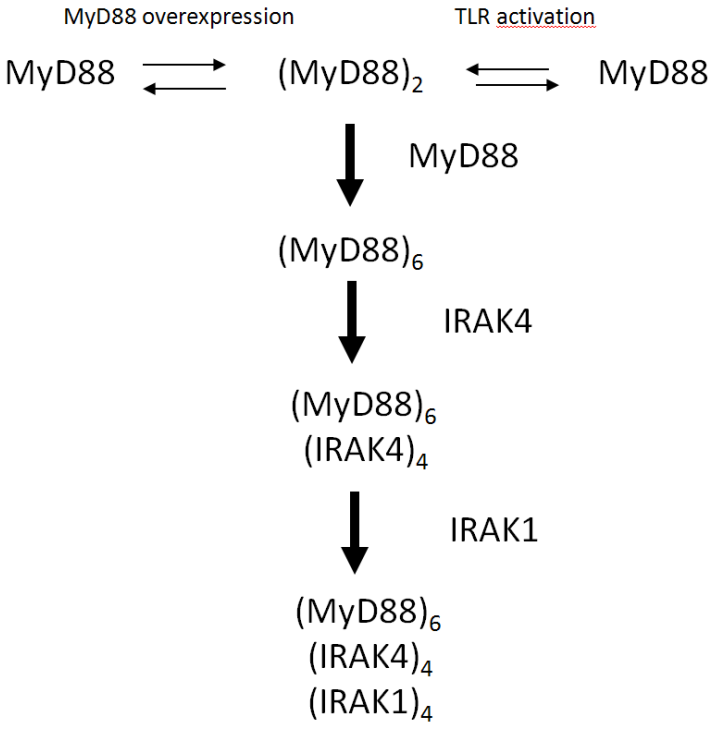

Figure S10: The equilibrium between the monomeric and dimeric MyD88 which is in the is resting state biased towards the monomer is shifted to the dimeric form by interaction with activated TLRs or overexpression of MyD88, leading to the recruitment of additional MyD88 dimers $(MyD88)_6$ and to the assembly of Myddosome.

Supplemental figure S11

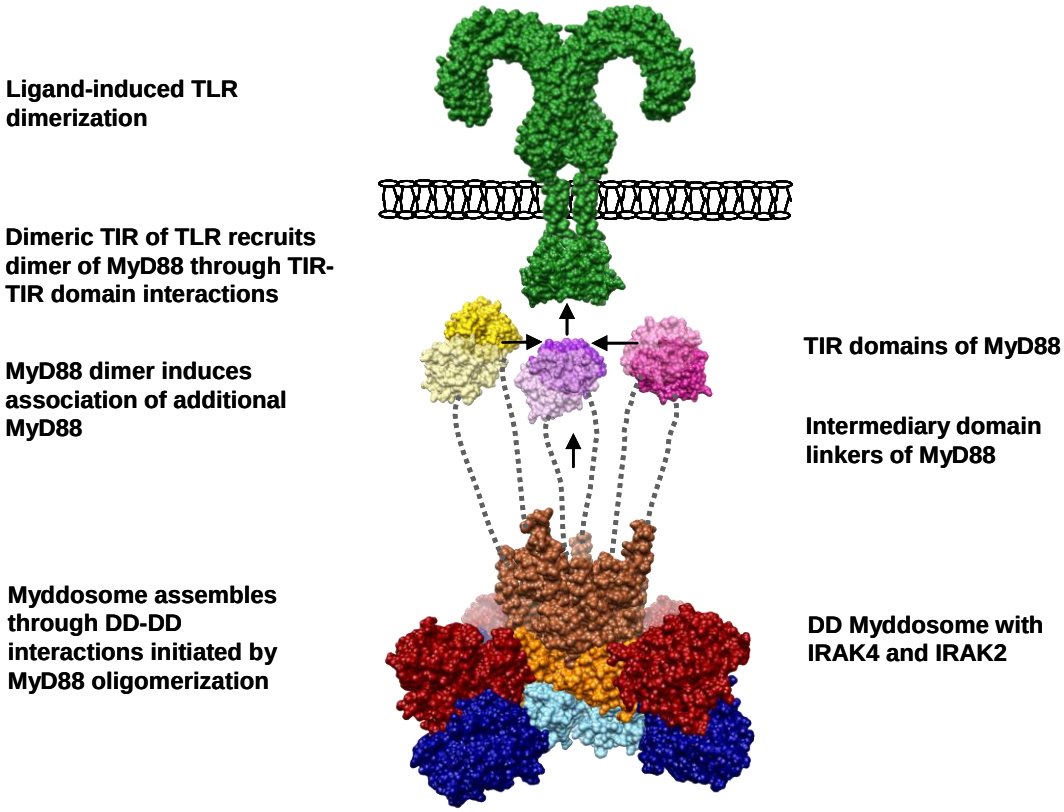

Figure S11: Molecular model representation of the activation of TLR signaling through the dimeric platform of TIR domains. TIR domain assembly was modeled by protein docking and is shown separated for clarity. TLRs, green (PDB code 3FXI for TLR4 ectodomains; PDB code 2J67 of dimeric TIR domains of TLR10); MyD88 TIR domains (PDB code 2Z5V) as dimers, violet, yellow and pink; Myddosome structure (PDB code 3MOP) -MyD88 DD, IRAK-4 DD, IRAK-2 DD, brown, orange, light blue; IRAK4 kinase domain, dark red (PDB code 2NRU); IRAK2 kinase domain, dark blue.